American Mineralogist, Volume 79, pages 848–861, 1994

The structural role of Mg in silicate liquids: A high-temperature ^{25}Mg, ^{23}Na, and ^{29}Si NMR study

Peter S. Fiske,* Jonathan F. Stebbins
Department of Geological and Environmental Sciences, Stanford University, Stanford, California 94305-2115, U.S.A.

Abstract

We have studied the structural role of Mg in silicate liquids as a function of temperature and composition using high-temperature ^{25}Mg, ^{23}Na, and ^{29}Si NMR. To establish the relationship between the isotropic chemical shift (δ_{iso}) and the coordination number for ^{25}Mg in silicates, we have obtained high-resolution ^{25}Mg MAS NMR spectra on isotopically enriched akermanite ($^{[4]}Mg$) and diopside ($^{[6]}Mg$) using spin-echo pulse sequences and absolute-value Fourier-transform techniques. The δ_{iso} for akermanite is 49 ± 3 ppm, and that for diopside is 8 ± 3 ppm, demonstrating that the chemical-shift range for ^{25}Mg in the silicates is similar to that established in oxides.

The δ_{iso} for ^{25}Mg in $(CaO)_{0.29}(MgO)_{0.14}(SiO_2)_{0.57}$ liquid at 1400 °C is 8 ppm, suggesting that Mg resides in a structural environment similar to that in diopside. The δ_{iso} for ^{25}Mg in $(Na_2O)_{0.28}(MgO)_{0.18}(SiO_2)_{0.54}$ liquid shifts from 34 ppm at 1150 °C to 29 ppm at 1360 °C, indicating smaller coordination numbers than in the Ca liquid but a relatively large increase in the Mg-O bond length or coordination number (or both) with increasing temperature. The δ_{iso} for ^{23}Na shows similar, but less pronounced, changes, whereas the ^{29}Si δ_{iso} is unchanged over this range of temperatures. This suggests that Mg undergoes the largest increases in bond distance or CN (or both) of any of the cations in the liquid.

Spin-lattice relaxation times for ^{25}Mg and ^{23}Na were measured in liquid $(Na_2O)_{0.28}$-$(MgO)_{0.18}(SiO_2)_{0.54}$ over the same range of temperatures. The apparent activation energy of the ^{25}Mg relaxation (related to Mg diffusional motion) is 119 kJ/mol, intermediate between that of Na and Si. The apparent activation energy for ^{23}Na relaxation is 85 kJ/mol, which is higher than that observed in sodium silicate liquids of similar polymerization but comparable to that in mixed alkali silicate liquids, suggesting that Na and Mg may show a mixed-cation effect.

Introduction

The structure and dynamical properties of silicate liquids exert a fundamental control on igneous processes such as mineral-melt equilibrium, elemental partitioning, and transport properties, including diffusion, viscosity, and density. Although much is known about silicate minerals, relatively little is known about the liquids from which these minerals form. Much of our existing knowledge about silicate liquids is based on inferences made from studies of macroscopic properties such as those mentioned above, but these inferences can be nonunique. Thus, direct studies of the structure of silicate liquids at high temperature hold great promise for elucidating the physics and chemistry of natural magmas.

Most information about the structure of silicate liquids has come from the study of silicate glasses, the structures of which represent that of the liquid at the glass-transition temperature. There are obvious limitations to this approach. First, the kinetics of structural relaxation in silicate liquids makes it difficult to quench glasses with fictive temperatures differing by >100 °C or so (Brandriss and Stebbins, 1988; Dingwell and Webb, 1990). This range in temperature is often too small to discern temperature-dependent changes in liquid structure. Furthermore, low-silica liquids cannot be easily quenched to glasses. And, by definition, the dynamical phenomena that control the transport properties in silicate liquids are not observable below the glass-transition temperature. To link the large body of data from glasses to those data measured at high temperature (and to magmatic conditions), it is critical to understand how the structure of silicate liquids changes with temperature.

Recently, several spectroscopic techniques have been adapted to study the structure of silicate liquids at high temperature. They include X-ray techniques (XANES, EXAFS: Waychunas et al., 1988; Jackson et al., 1993; Brown et al., 1993), vibrational spectroscopies (McMillan et al., 1992; Mysen and Frantz, 1992), and nuclear magnetic resonance (NMR) spectroscopy (Stebbins, 1988, 1991; Coutures et al., 1990; Coté et al., 1992). They have

* Present address: Institute of Geophysics and Planetary Physics, Lawrence Livermore National Laboratory, L-413, Livermore, California 94550, U.S.A.

0003–004X/94/0910–0848$02.00

allowed for the investigation of the structure of silicate liquids over a wider range of temperatures and at temperatures of relevance to magmatic processes.

Mg is a major constituent in most magmas, and, in primitive, undifferentiated magmas, it can be the most abundant oxide after silica. Mg also represents an important group of cations, such as Ca^{2+}, Fe^{2+}, Co^{2+}, and Ni^{2+}, whose size and charge are intermediate between those of network-forming cations such as Si^{4+}, Al^{3+}, and Fe^{3+} and the charge-balancing, large, monovalent cations such as the alkalis.

There have been a number of spectroscopic and theoretical investigations of the structure of Mg-bearing silicate glasses and liquids. They include X-ray scattering (Waseda and Toguri, 1977; Yin et al., 1983), X-ray emission and molar refractivity (Hanada et al., 1988), vibrational spectroscopies (McMillan, 1984; Williams et al., 1989; Cooney and Sharma, 1990; Kubicki et al., 1992), and molecular dynamics (MD) simulations (Matsui et al., 1982; Dempsey et al., 1984; Kubicki and Lasaga, 1991). Most of these studies conclude that Mg^{2+} resides in a distorted site; however, disagreement exists regarding the actual coordination number for Mg^{2+}.

The possibility of multiple coordination environments for Mg^{2+} in silicate liquids and glasses is suggested by EXAFS studies of divalent cations of similar radius. Fe^{2+} and Ni^{2+} EXAFS studies show dominantly tetrahedral coordination of these cations in a number of silicate liquids and glasses studied (Waychunas et al., 1988; Jackson, 1991; Galoisy and Calas, 1991, 1992, 1993a, 1993b; Brown et al., 1993; Farges et al., 1993, 1994). Those studies suggested that Mg^{2+}, being intermediate in size between Fe^{2+} and Ni^{2+}, may also assume a tetrahedral coordination in silicate liquids.

The high heat capacities and thermal expansivities of silicate liquids require that they undergo continuous structural changes with temperature, which may include changes in the coordination of cations (e.g., Richet and Neuville, 1992). Recent heat capacity measurements of magnesium aluminosilicate liquids have demonstrated a simple linear relationship between configurational heat capacity and Si/(Mg + Al) over an extremely wide range of composition, implying that the structural changes with temperature are mainly due to short-range O to cation interactions (Courtial and Richet, 1993). The high partial molar heat capacity of MgO in silicate liquids indicates that Mg^{2+} may undergo particularly large configurational changes in silicate liquids as a function of temperature (Stebbins et al., 1984; Richet and Neuville, 1992). Furthermore, studies of glasses and liquids in the systems diopside-albite and diopside-anorthite have documented excess enthalpies of mixing in the liquids that are substantially more positive than in the glasses (Stebbins et al., 1984; Navrotsky et al., 1989). This excess enthalpy probably reflects a greater number of structural configurations in these liquids (Stebbins et al., 1984) and may be due to mixing of Mg on tetrahedral, as well as octahedral, sites.

This study represents the first application of ^{25}Mg NMR to silicate liquids at high temperature, with the goal of determining the structural environment of Mg as a function of temperature and composition. Because so little is known about the NMR chemical shifts for ^{25}Mg in solids, it was also necessary to study several model compounds with known structures. Our success in observing NMR signals in silicate liquids at high temperature suggests that NMR studies of other nuclides that are difficult to observe such as $^{47,49}Ti$ and ^{43}Ca may also be possible.

Experimental procedures

The samples used in this study were synthesized using reagent-grade oxides and carbonates. The ^{25}Mg isotopically enriched samples were made using 99% ^{25}Mg–enriched MgO powder (Oak Ridge National Laboratory). The crystalline compounds were synthesized with 0.2 wt% Co^{2+} added to speed spin-lattice relaxation. Samples were synthesized at high temperature in air using Pt or PtAu crucibles. Careful weight-loss measurements confirmed that alkali loss was insignificant and that desired stoichiometries were reached.

Crystalline akermanite ($Ca_2MgSi_2O_7$)

The reagent mixture was heated to 1300 °C at 200 °C/h, held for 12 h, quenched, reground, and annealed at 1300 °C for 20 h. XRD spectra for this sample showed only peaks for akermanite. The powders were deep blue due to the $^{[4]}Co^{2+}$ dopant (e.g., Rossman, 1988; Keppler, 1992). The ^{29}Si MAS NMR spectra of this sample showed a single asymmetric peak centered at −76.4 ppm, representing the Si site in akermanite (Janes and Oldfield, 1985), and a small peak centered at −84.4 ppm, probably representing diopside (<2% by area) (Smith et al., 1983).

Crystalline diopside ($CaMgSi_2O_6$)

The reagent mixture was heated to 1300 °C at 200 °C/h, held for 12 h, quenched, reground, and annealed at 1300 °C for 24 h. XRD spectra of this sample showed it to contain only diopside. The powder was light pink, consistent with the $^{[6]}Co^{2+}$ dopant (e.g., Rossman, 1988). The ^{29}Si MAS NMR spectra of this sample showed a single symmetric peak centered at −84.4 ppm, consistent with previous data (Smith et al., 1983). The width of this peak, 3.4 ppm, is considerably broader than that observed for most crystalline silicates, suggesting that this sample may contain significant structural disorder.

Magnesium silicate glasses containing Na, K, and Ca

Glasses of the compositions detailed in Table 1 were all prepared with ^{25}Mg isotopically enriched MgO powder. No paramagnetic dopant was used for these materials. The reagent mixtures were slowly heated to temperatures above the decarbonation point for the respective alkali or calcium carbonates, held for 4 h, then heated at 300 °C/h to 50 °C above their respective melting points, held for 30 min, and then quenched by placing the bottom of the crucible in a shallow dish of H_2O. Inspection

TABLE 1. Compositions of silicate liquids in this study

Composition	Name	NBO/T	Liquidus *T*	Reference
$(Na_2O)_{0.2}(MgO)_{0.2}(SiO_2)_{0.60}$	NaMg1	1.3	915 ± 5 °C	Schairer, 1957
$(Na_2O)_{0.28}(MgO)_{0.18}(SiO_2)_{0.54}$	NaMg2	1.73	840 ± 10 °C	Schairer, 1957
$(K_2O)_{0.29}(MgO)_{0.14}(SiO_2)_{0.57}$	KMg1	1.5	1100 ± 30 °C	Roedder, 1951
$(CaO)_{0.29}(MgO)_{0.14}(SiO_2)_{0.57}$	CaMg1	1.5	1325 ± 10 °C	Schairer and Bowen, 1942

of the products under high magnification and with crossed polars showed the glasses to have no detectable crystals or unreacted material. After the high-*T* NMR experiment, the $(Na_2O)_{0.28}(MgO)_{0.18}(SiO_2)_{0.54}$ glass (from now on referred to as NaMg2) was reground and doped with 0.2 wt% Co^{2+} and revitrified. The resulting glass appeared dark blue, indicating that the Co^{2+} resided at least partially in tetrahedral coordination.

NMR spectral acquisition procedures

The ^{25}Mg MAS NMR spectra were acquired using a Varian VXR-400S NMR spectrometer operating at a Larmor frequency of 24.512 MHz for ^{25}Mg with a Doty Scientific probe. The ^{25}Mg chemical shifts were calibrated against an external 1-*M* $Mg(NO_3)_2$ aqueous solution. The liquid 90° pulse length measured on this standard was about 30 μs. Samples were contained in a 5-mm diameter sapphire rotor and spun at about 9500 Hz. The spectral width was 100 kHz, and the digital resolution was 6 Hz. Probe ringing required a dead time of about 85 μs prior to acquisition.

The ^{29}Si MAS NMR spectra of the crystalline compounds and the NaMg2 glass doped with 0.2 wt% Co^{2+} were acquired at a Larmor frequency of 79.459 MHz using a Varian MAS probe with a ZrO_2 rotor spinning at 5500 Hz. The ^{29}Si chemical shifts were referenced to an external standard (tetramethyl silane) contained in an identical rotor. The average isotropic chemical shift for the ^{29}Si in the glass was determined by measuring the integral of the central transition and the first set of sidebands (the sidebands represented about 10% of the total signal), determining the center of gravity of each, and then taking the weighted average over the entire spectrum. Several repetitions of this procedure yielded values with a range of ±0.5 ppm.

The ^{25}Mg NMR spectra are difficult to obtain because of the low natural abundance (10.16%) and low resonance frequency of ^{25}Mg, which greatly reduces the sensitivity. In addition, the second-order quadrupolar broadening of the central transition is roughly nine times greater than for ^{27}Al in an identical site (Dupree and Smith, 1988). Good results for both akermanite and diopside were obtained on ^{25}Mg isotopically enriched samples using a single pulse with an rf tip angle of about 20–30°, a delay of 0.1 s, and roughly 100 000 signal averages. However, spin-echo techniques (see next section) yielded somewhat improved results for the enriched materials and were used to determine the isotropic chemical shifts.

The NMR values, δ_{iso} (isotropic chemical shift), C_q (the quadrupolar coupling constant, equal to e^2qQ/h), and η (the asymmetry parameter), for ^{25}Mg in the crystalline materials were determined in two ways. The quadrupolar coupling constant can be determined by measuring the difference between the centers of gravity of the central ½-½ transition and the outer ±½-±3/2 and ±3/2-±5/2 transitions (Lippmaa et al., 1986; see Hovis et al., 1992, for an example), and δ_{iso} can be estimated. Alternatively, the spectra can be simulated directly, yielding values for δ_{iso}, C_q, and η. The simulation algorithm used for this study is based on the procedure of Müller (1982). The best fit of the spectra was achieved by visual inspection to maximize the positions of discontinuities in the line shapes rather than least-squares minimization of the entire spectrum because these features are less affected by distortions of the spectra. The estimated uncertainty is also based on the visual comparison of the fit with a range of values for each NMR parameter.

Application of Hahn spin-echo pulse sequence and absolute-value spectra

For broad NMR peaks, it is difficult to acquire undistorted spectra using single-pulse techniques. That is because the first part of the FID (free induction decay) includes the information about the broadest components to the NMR line shape. This information can be lost in the time between applying the excitation pulse and turning on the receiver to acquire the FID. In the case of low-frequency nuclides such as ^{25}Mg, this problem can be worse because probe ringing can severely distort the first part of the FID, necessitating further truncation of the data.

More complex pulse sequences can be used to reduce, or even eliminate, these problems. The Hahn spin-echo pulse sequence (90°-τ-180°) can be particularly useful. The 90° pulse tips the magnetization of the sample into the **x-y** plane, and after a time τ, the 180° pulse is applied. The 180° pulse reorients the magnetization so that, instead of drifting out of phase, the individual spins rephase after a time 2τ. This rephasing produces an echo in the FID, with the top of the echo representing the point at which the spins fall completely in phase. Thus, a Fourier transform of the FID starting at the top of the echo yields a complete NMR signal, free from distortions due to truncations of the FID and due to probe ringing.

Recently, Grandinetti et al. (1993) have developed an improvement to this technique. Rather than truncating the FID at the top of the echo, they used the entire echo in the Fourier transform. The resulting spectrum can thus be displayed in absolute-value mode, where each point of the displayed spectrum is calculated as the square root of the sum of the squares of the real and imaginary com-

ponents of each complex data point. This results in a complete elimination of the base-line rolls because of phasing problems and increases the signal to noise of the spectrum by roughly a factor of $\sqrt{2}$ (Grandinetti et al., 1993). In addition, the spinning sidebands are greatly diminished. A comparison of the spectra for diopside acquired with a single pulse vs. a Hahn spin echo with absolute-value full-echo transform is presented in Figure 1. The best-fit simulations of the central transitions for the two spectra yielded somewhat different values for the isotropic chemical shift and indicated that neither is completely free of distortion. Both kinds of spectrum show peaks and shoulders at the same frequencies, but the Hahn spin-echo spectra generally have much narrower peak widths than the single-pulse spectra. Although the signal to noise ratios for the Hahn-echo spectra are improved, they are lower in absolute intensity by roughly a factor of 2. That may be because of the removal of the paramagnetically broadened component of the NMR signal, which may not refocus during the echo and which can distort the single-pulse spectra.

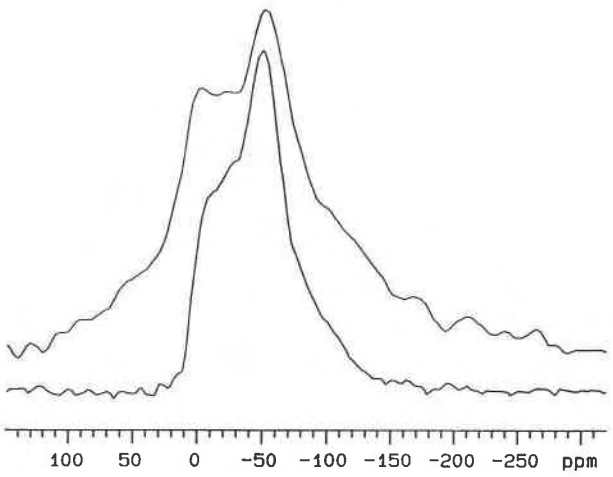

Fig. 1. The ^{25}Mg MAS NMR single-pulse and Hahn-echo spectra for crystalline diopside doped with 0.2 wt% Co^{2+}. The Hahn-echo spectrum is substantially narrower than the single-pulse spectrum and yields an isotropic chemical shift of 8 ± 4 ppm, whereas the single-pulse spectrum yields a value of 22 ± 5 ppm.

^{25}Mg and ^{23}Na relaxation times

For quadrupolar nuclei, spin-lattice relaxation is usually caused by fluctuations in the electric field gradient around the nucleus. In liquids, especially silicate liquids at high temperature, these fluctuations are often caused by the diffusional motion of the resonating atom (e.g., Liu et al., 1987, 1988). Relaxation is most efficient, and T_1 is shortest, when these motions are at the Larmor frequency. When molecular motion is either much slower or much faster than the Larmor frequency, relaxation is less efficient and T_1 is longer. In those regions away from the T_1 minimum, the rate of change of the relaxation time with temperature can yield an apparent activation energy that may characterize the motion responsible for relaxation (reviewed by Stebbins, 1988).

At temperatures well above the T_1 minimum, the width of the NMR peak is generally controlled by the spin-lattice relaxation time where $T_2 = 1/(\pi\nu_{1/2})$ and $T_1 = T_2$. T_2 is the spin-spin relaxation time, and $\nu_{1/2}$ is the width of the peak at half height in hertz. To confirm that that condition held for our experiments, the spin-lattice relaxation time was measured directly at 1263 °C using the inversion recovery technique (e.g., Fukushima and Roeder, 1981). A nonlinear least-squares regression of the peak intensity vs. delay time was used to calculate the relaxation time T_1. The measured T_1 matched that predicted from the line width to within 5%.

^{25}Mg CHEMICAL SHIFTS AND SITE INFORMATION IN CRYSTALLINE SOLIDS

Few data have been published on ^{25}Mg chemical shifts in solids (e.g., MacKenzie and Meinhold, 1994a, 1994b). The ^{25}Mg data show the same trend to increasing chemical shielding with increasing coordination number as other cations such as Si, Al, and Na. The range in chemical shift between $^{[4]}$Mg (in $MgAl_2O_4$) and $^{[6]}$Mg (in MgO) is 26 ppm (Dupree and Smith, 1988), compared with approximately 100 ppm for ^{29}Si in fourfold and sixfold coordination, 60 ppm for ^{27}Al in fourfold and sixfold coordination (Engelhardt and Michel, 1987), and 20 ppm for ^{23}Na in sixfold and eightfold coordination (Xue and Stebbins, 1993). However, second-nearest-neighbor effects on the isotropic chemical shift may be larger for cations with a lower charge. In the case of ^{23}Na, the degree of polymerization has nearly as large an effect on δ_{iso} as the coordination number (Xue and Stebbins, 1993). Therefore, the limited amount of ^{25}Mg chemical shift information available from oxides might not be easily applied to silicates because of differences in second-nearest-neighbor populations. Thus, it was necessary to study Mg-bearing silicate minerals with different Mg coordinations and compare their isotropic chemical shifts with those known for the oxides.

There are several constraints limiting the choice of model compounds for the calibration of ^{25}Mg NMR chemical shifts in silicates. The magnitude of the quadrupolar coupling (C_q) for quadrupolar nuclides in solids is proportional to the distortion of the atomic site (Ghose and Tsang, 1973). Because of the substantial effect of second-order quadrupolar broadening for ^{25}Mg, we selected minerals with the most regular Mg sites. Composition places additional constraints: the minerals cannot contain more than a few percent of paramagnetic cations such as Fe^{2+} because of problems with paramagnetic broadening, and the proportion of SiO_2 to the other cations must not differ too much from that of the liquids of this study. The minerals akermanite ($Ca_2MgSi_2O_7$) and diopside ($CaMgSi_2O_6$) were the best match to these criteria. The site information for Mg in these two minerals, as well as in the oxides, is summarized in Table 2.

The ^{25}Mg MAS NMR Hahn-echo spectrum for aker-

TABLE 2. Site information for Mg in the oxides and silicates studied

Mineral	Mg-O bond length (Å)	Bond length variation	O-Mg-O angle variation	CN of Mg	CN of O linked to Mg	Isotropic chemical shift (ppm)
Periclase (MgO)	2.105	0	0	6	6 (all Mg)	25
Spinel ($MgAl_2O_4$)	1.924	0	0	4	4 (3Al,Mg)	52
Diopside ($CaMgSi_2O_6$)	2.077	1%	17.4°	6	3,4 (Mg,Ca,Si ± Mg)	8 ± 3
Akermanite ($Ca_2MgSi_2O_7$)	1.915	0	5.8°	4	4 (Mg,Si,Ca,Ca)	49 ± 4

Note: site information is from Smyth and Bish (1988). CN = coordination number.

manite, along with a simulation of the central transition, is shown in Figure 2. The central peak consists of a broad doublet consistent with an asymmetry parameter of 0.2–0.3, a quadrupolar coupling constant of 2.7–2.9 MHz, and an isotropic chemical shift between 47 and 52 ppm. The extra intensity to higher frequency may represent a small amount of distortion of the spectrum. Analysis of the centers of gravity of the spinning sidebands in the single-pulse spectrum suggests a quadrupolar coupling constant of 2.9–3.0 MHz.

The ^{25}Mg MAS NMR Hahn-echo spectrum for diopside, along with a simulation of the central transition, is shown in Figure 3. The central peak has a small, high-frequency shoulder. The central peak is best simulated with an asymmetry parameter of 1–0.8, a quadrupolar coupling constant of 2.0 ± 0.05 MHz, and an isotropic chemical shift of 8 ± 3 ppm. Analysis of the centers of gravity of the spinning sidebands in the single-pulse spectrum suggests a quadrupolar coupling constant of 2.2 MHz.

In comparison, the single-pulse spectrum for diopside (Fig. 1) has additional intensity at high and low frequency and has a wider line width overall. The best-fit simulation of this spectrum has an asymmetry parameter of 1–0.8, a quadrupolar coupling constant of 2.3 ± 0.1 MHz, and an isotropic chemical shift of 22 ± 3 ppm. The high-frequency shoulder is present in both spectra and may represent the center of the ±½-±⅔ transition, although it is centered slightly lower in frequency than that expected from the sideband analysis. It is unlikely that the peak represents Mg on the larger M2 site in diopside (occupied by Ca), as this would be expected to produce a peak at lower frequency because of the longer bond lengths and higher coordination number for this site.

The differences in chemical shift between the silicates studied and those known for the oxides can be explained using empirical trends established for other cations. Both silicates have a lower chemical shift (greater chemical shielding) than the respective oxides with the same coordination number for Mg. This follows the trend found for ^{27}Al and ^{29}Si, where increasing the number of Si next-nearest neighbors causes increased shielding (Engelhardt and Michel, 1987; Kirkpatrick, 1988). The much larger difference in chemical shift between periclase and diopside than between spinel and akermanite reflects the fact that the two minerals with $^{[6]}$Mg have larger differences in their next-nearest-neighbor populations than do the two minerals with $^{[4]}$Mg. In the case of periclase, the O atoms around the Mg are sixfold coordinated, whereas in diopside they are threefold and fourfold coordinated. In contrast, the O atoms around Mg in akermanite and spinel are both fourfold coordinated.

Arguments such as these can also illustrate the difficulty in interpreting chemical shift data in terms of specific structural parameters. For example, as stated earlier, increasing Mg coordination (which necessitates an increase in the average bond length) corresponds to an increase in shielding (decreased chemical shift). However, within each pair of minerals, those with shorter bonds (the silicates) actually have a lower chemical shift. Whereas the current paucity of data prevents a more complex analysis of chemical shift trends, ^{25}Mg chemical shifts will likely show the same complex relationship to bond length, bond angle, second-nearest-neighbor population, and other structural parameters as do other NMR nuclides.

In conclusion, the chemical shift trend for Mg in different coordination environments in the two silicates does not differ greatly from the trend observed in the two oxides, and like ^{27}Al and ^{29}Si, coordination number exerts a primary control on ^{25}Mg chemical shifts in solids. This enables us to make some limited structural inferences for Mg in the silicate liquids on the basis of their observed isotropic chemical shifts.

HIGH-TEMPERATURE ^{25}Mg NMR IN SILICATE LIQUIDS

Observation of a signal from ^{25}Mg in silicate liquids at high temperature that represents the average isotropic chemical shift is dependent on several related factors. First, the viscosity of the liquid must be sufficiently low to allow for rapid isotropic reorientation of the local environment around the resonating nuclide. This averages out the entire spectrum for all the transitions (usually several megahertz in width) and results in a sharp, resolvable NMR peak, the position of which represents the isotropic (true) chemical shift for the site. For network-forming cations such as Si and Al, the reorientation frequency can be crudely estimated from the viscosity using the Maxwell equation for viscoelastic behavior: $\tau = \eta/G_\infty$ (e.g., Dingwell and Webb, 1989), where τ is the shear relaxation time, η is the viscosity in pascal seconds, and G_∞ is the infinite frequency shear modulus. However, for cations that are not strongly bound to the silicate network, such as the alkalis, hopping frequencies are not correlated with viscosity but must be estimated using data for tracer diffusivities or other transport properties (e.g.,

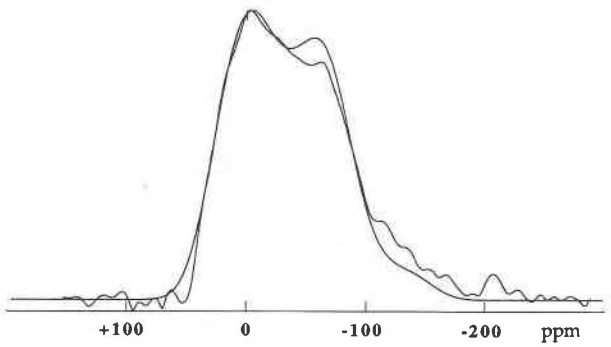

Fig. 2. The ^{25}Mg MAS NMR Hahn-echo spectrum for akermanite. The central ½-½ transition is best fit with a δ_{iso} of 49 ± 3 ppm, a C_q of 2.8 ± 0.1 MHz, an asymmetry parameter of 0.2–0.3, and a line broadening of 900 Hz.

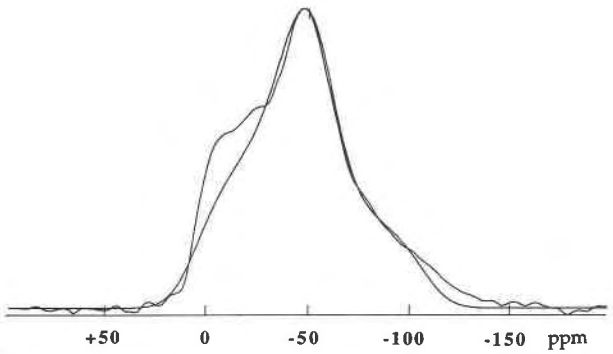

Fig. 3. The ^{25}Mg MAS NMR Hahn-echo spectrum for diopside. The central ½-½ transition is best fit with a δ_{iso} of 8 ± 3 ppm, a C_q of 2.0 ± 0.05 MHz, an asymmetry parameter of 0.9–1.0, and a line broadening of 600 Hz.

Liu et al., 1987, 1988). In the case of Mg, for which tracer diffusion data are lacking, the Maxwell equation provides an initial estimate that is likely to be a lower bound only. For quadrupolar nuclides such as ^{25}Mg, the static NMR powder pattern for all the $2I$ transitions (where I is the nuclear spin, in this case ½) can span several megahertz. Full averaging is achieved at hopping frequencies on the order of tens of megahertz, which, using the Maxwell equation, correspond to viscosities of $<10^2$ Pa·s.

Another constraint is the relaxation time (T_1) for ^{25}Mg in the liquid. For an NMR signal to be observable, T_1 must fall into a certain range. Relaxation times must be short enough to allow efficient data collection; the low sensitivity for the nuclide requires a minimum of thousands of signal averages. However, if the T_1 is too short, the line width increases, reducing the ratio of signal to noise. If T_1 falls below tens of microseconds, the signal may be lost entirely in the instrumental dead time.

Results for liquids

The composition of the calcium magnesium silicate liquid [composition $(CaO)_{0.29}(MgO)_{0.14}(SiO_2)_{0.57}$, hereafter referred to as CaMg1] chosen for this study (Table 1) falls along the eutectic between tridymite and diopside, with an estimated melting temperature of 1325 °C (Schairer and Bowen, 1942). The ^{25}Mg NMR signals were observed at 1350 and 1400 °C (Fig. 4). The peaks were fitted to single Lorentzian line shapes, which yielded peak positions of 5 ± 15 and 8 ± 3 ppm, respectively. The decrease in the line width with increase in temperature indicates that the ^{25}Mg T_1 in this liquid is increasing with temperature and that these temperatures lie above that of the T_1 minimum.

Two compositions in the system Na_2O-MgO-SiO_2 were studied at high temperature, along with a single composition in the system K_2O-MgO-SiO_2 (Table 1). No signal was observable in the $(Na_2O)_{0.2}(MgO)_{0.2}(SiO_2)_{0.60}$ liquid (hereafter referred to as NaMg1) up to 1310 °C or in the $(K_2O)_{0.29}(MgO)_{0.14}(SiO_2)_{0.57}$ (hereafter referred to as KMg1) up to 1290 °C, possibly because of the extremely short T_1 for ^{25}Mg in these liquids and correspondingly broad peaks.

However, the NaMg2 liquid yielded observable NMR signals from 1119 to 1368 °C (Fig. 5). The peaks were fitted to single Lorentzian lines to determine the peak position and line width at each temperature. The peak positions are plotted in Figure 6. The narrowing of the NMR peak with increasing temperature indicates that, like the calcium silicate liquid, the temperatures at which these spectra were obtained lie above the T_1 minimum for ^{25}Mg in the liquid. To confirm that the line widths are actually controlled by the T_1, the latter was measured directly at two temperatures using the techniques described above. The T_1 measured matched those estimated from the line widths to within 5%. The derived activation energy for the mechanism of ^{25}Mg relaxation (119 ± 8 kJ/mol) was determined by calculating the least-squares fit to the slope of the relaxation time data vs. temperature on an Arrhenius plot (Fig. 7).

Both ^{29}Si NMR and ^{23}Na NMR spectra were also obtained for this sample over the same range in temperature. As with the ^{25}Mg results, the ^{29}Si and ^{23}Na peaks were fitted with single Lorentzian line shapes, and the peak position and line widths were determined. The isotropic chemical shifts vs. temperature for ^{29}Si and ^{23}Na are plotted in Figure 8. The ^{23}Na relaxation times were derived in the same manner as for ^{25}Mg and are plotted on an Arrhenius plot as well (Fig. 9). The derived activation energy for the ^{23}Na relaxation is 85 ± 10 kJ/mol.

No ^{25}Mg NMR signal was observable from the doped NaMg2 glass using single-pulse MAS techniques at room temperature, probably because of severe quadrupolar or paramagnetic broadening. However, using the Hahn-echo sequence, a weak broad peak (centered at −20 ppm, and 200 ppm wide) was detected after 10000 signal averages. Its low intensity clearly showed that only a fraction of the ^{25}Mg signal was detected.

Discussion

Previous spectroscopic and molecular dynamics studies of magnesium silicate liquids and glasses

Previous theoretical and spectroscopic studies in Mg in silicate liquids have principally focused on $MgSiO_3$ and Mg_2SiO_4 glasses and liquids (Table 3). These studies (see

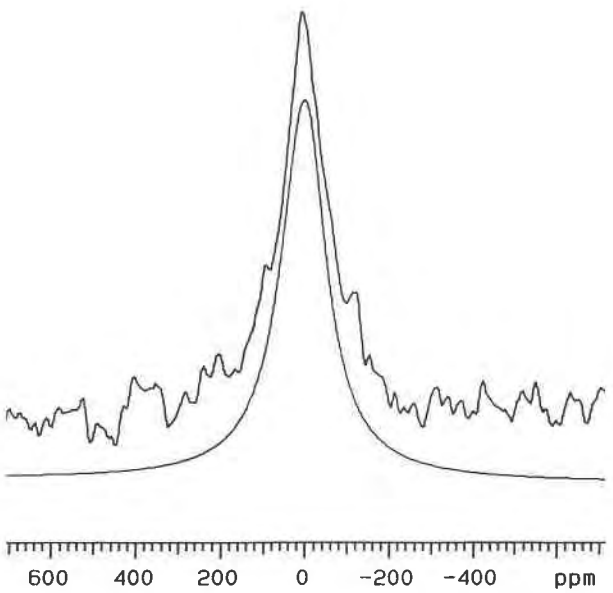

Fig. 4. The ^{25}Mg NMR spectrum for CaMg1 liquid at 1400 °C. The single peak is fitted with a Lorentzian line shape at 8 ± 3 ppm.

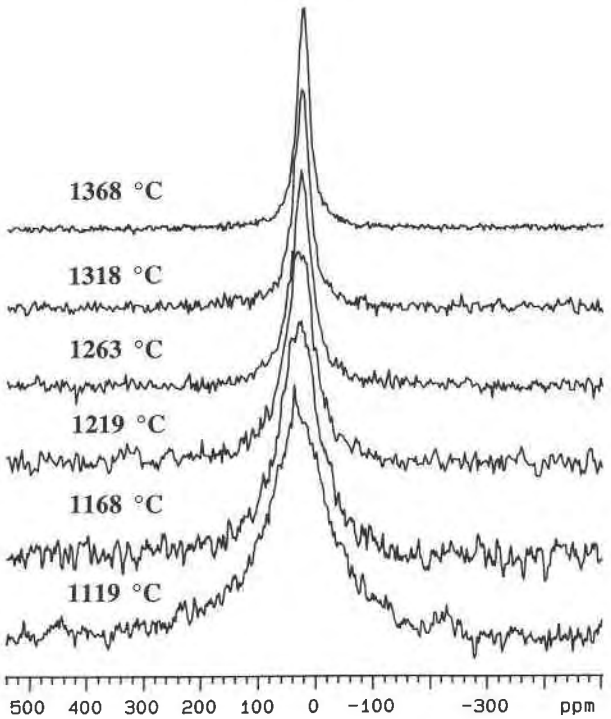

Fig. 5. The ^{25}Mg NMR spectra for NaMg2 liquid from 1119 to 1368 °C. The narrowing of the peak with increasing temperature indicates that these temperatures are above that for the T_1 minimum.

also Navrotsky et al., 1985) suggest that the local structural environment around Mg is different in these two liquids.

$MgSiO_3$. X-ray scattering studies (Waseda and Toguri, 1977; Waseda, 1980) determined the mean Mg-O bond length to be 2.14 Å in enstatite glass and 2.16 Å in the liquid at 1700 °C and reported a mean coordination number of 4.5. However, Yin et al. (1983) proposed the mean coordination number of Mg to be 6, on the basis of fitting their X-ray scattering data to a quasi-crystalline model for the glass. Early molecular dynamics (MD) simulations by Matsui et al. (1982) yielded simulated RDF patterns that were similar to those observed in the previous X-ray scattering studies and reported a mean Mg-O bond length of 2.1 Å. However, more recent MD simulations by Kubicki and Lasaga (1991) disagree with the interpretations of Yin et al. (1983) and suggest a mean Mg-O bond distance of 1.9 Å, corresponding to a mean coordination number for Mg close to 4. However, it should be noted that both MD simulations correspond to extremely high fictive temperatures (roughly 5000 and 2000–5000 K, respectively) and may not be directly comparable with spectroscopic studies of glasses (with fictive temperatures of roughly 1000 K). A relatively low abundance of $^{[6]}$Mg in enstatite glass is further implied by Raman spectra of glasses in the system $MgSiO_3$-$CaSiO_3$, which show a progressive loss of a low-frequency peak associated with $^{[6]}$Ca or $^{[6]}$Mg with increasing Mg content (Kubicki et al., 1992). Finally, X-ray emission spectra and molar refractivity measurements of rf-sputtered amorphous films in the system MgO-SiO_2 indicate predominantly tetrahedral coordination of Mg when the MgO content is 50% or less (Hanada et al., 1988).

Mg_2SiO_4. The local environment of Mg^{2+} in forsterite glass seems to be significantly different from that in enstatite glass and liquid. MD simulations (Matsui et al., 1982) proposed higher coordination numbers and longer Mg-O bond distances in forsterite liquids when compared with enstatite liquids. In addition, vibrational spectroscopic studies (Williams et al., 1989; Cooney and Sharma, 1990) show that, unlike in the enstatite-wollastonite system, Ca and Mg substitute freely in the orthosilicate system, suggesting that Mg^{2+} is principally octahedrally coordinated, whereas Fe^{2+}, which is dominantly tetrahedrally coordinated in these glasses (Jackson et al., 1993), does not substitute freely for Mg^{2+}.

^{25}Mg chemical shifts and coordination number

As outlined earlier, it is difficult to make unique structural interpretations from NMR chemical shift data because chemical shielding is a complex function of many structural parameters such as bond length, bond angle, and coordination number, which are themselves interrelated. The trend to lower chemical shift (increased shielding) with increased coordination number is well established for ^{29}Si, ^{27}Al, ^{23}Na, and the limited set of data from this study, ^{25}Mg. This is commonly ascribed to an increase in the ionicity of the M-O bond with increasing bond length, which increases the positive charge on the cation and thus the overall chemical shielding (Engelhardt and Michel, 1987). Calculations of the variation of chemical shielding with structural parameters for simple silicate molecules confirm that increased Si-O bond dis-

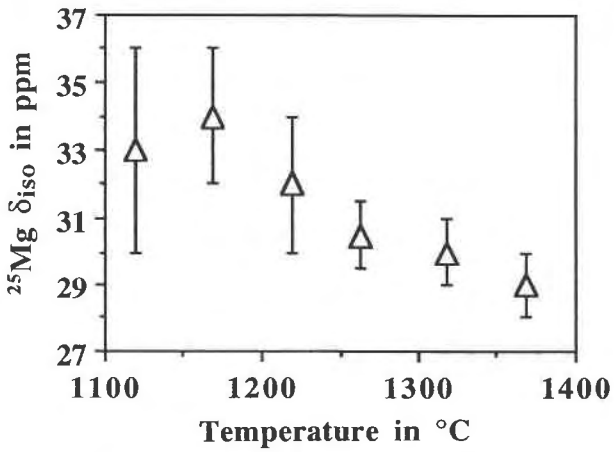

Fig. 6. The ^{25}Mg chemical shifts for NaMg2 liquid as a function of temperature.

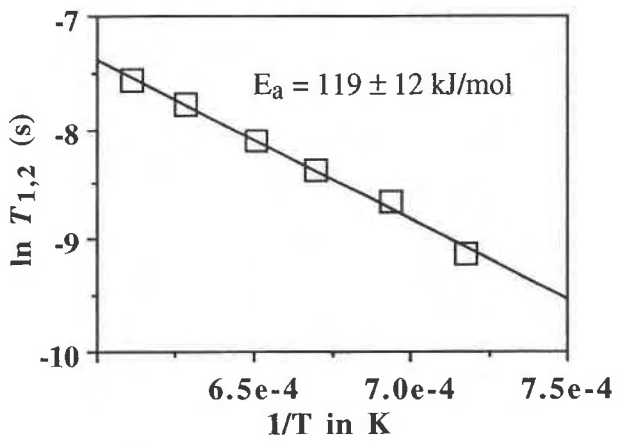

Fig. 7. The ^{25}Mg relaxation time data vs. temperature. An Arrhenius fit to these data gives an activation energy of 119 ± 12 kJ/mol.

tances correspond to increased chemical shielding (Tossell and Lazzeretti, 1987; Lindsay and Tossell, 1991).

The ^{25}Mg chemical shift trends established from the oxide and silicate minerals summarized in Table 2 can be used to estimate the mean coordination number (and with less certainty, the mean Mg-O bond length) for Mg in the silicate liquids studied. The chemical shift for Mg in the calcium magnesium silicate liquid at 1400 °C is identical to that for Mg in diopside within the uncertainty of the measurement. This strongly implies that the Mg in this liquid at this temperature has a mean coordination of 6, with a mean Mg-O bond distance similar to that in diopside.

The alkali silicate liquid, however, has mean ^{25}Mg chemical shifts that are intermediate between sixfold and fourfold coordinations. This implies that the Mg in this liquid has an average coordination of about 5. Although we did not study any minerals (e.g., grandidierite, yoderite) with $^{[5]}$Mg to calibrate the position of pentahedrally coordinated Mg, the chemical shifts for $^{[5]}$Si and $^{[5]}$Al fall about midway between those for the more common fourfold- and sixfold-coordinated species (Stebbins and McMillan, 1993; Risbud et al., 1987). However, our results cannot distinguish between a dynamical average of $^{[4]}$Mg and $^{[6]}$Mg vs. $^{[5]}$Mg or a mixture of all three.

To compare the mean Mg-O bond distances in the silicate liquids of this study with those derived in previous studies, the chemical shift data summarized in Table 2 can also be used to estimate the correlation between ^{25}Mg chemical shifts and Mg-O bond distances. Clearly, this is an oversimplification and is difficult to constrain with the paucity of data from Mg-bearing minerals. Nevertheless, it does provide a means of comparing these results with previous work.

Using the data in Table 2, the ^{25}Mg chemical shift in the calcium magnesium silicate liquid correlates to a Mg-O bond distance of 2.08 Å at 1400 °C. The data for the alkali silicate liquid, when extrapolated to the same temperature, corresponds to a bond distance of about 2.00 Å.

We attribute the difference in bond length primarily to the replacement of Na for Ca, since the ratio of nonbridging O atoms to tetrahedral sites is similar for the two liquids. The trend to higher coordination numbers for Mg in the alkaline-earth silicate liquid vs. the alkali silicate liquid is similar to that observed for Ni^{2+} in glasses by EXAFS (Galoisy and Calas, 1992) and Ti^{4+} (Lange and Carmichael, 1987, 1990; Dingwell, 1992; Paris et al., 1993). This trend has been explained by the decrease in net charge on the coordinating O atom with increasing covalent bonding caused by the increased charge density of the modifying cation. The lowering of the charge on the O atom reduces the effect of anion repulsion and allows for larger coordinations. Stebbins and McMillan (1993) suggested that this effect may contribute to the

Table 3. Summary of previous studies of Mg^{2+} in glasses and liquids in the system MgO-SiO_2

Source	Material	Technique	Mg-O bond length
Waseda, 1980	$MgSiO_3$ glass	X-ray scattering	2.14 Å
Waseda, 1980	$MgSiO_3$ liquid	X-ray scattering	2.16 Å
Yin et al., 1983	$MgSiO_3$ glass	X-ray scattering	2.08 Å
Hanada et al., 1988	MgO-SiO_2 films	X-ray emission and molar refractivity	not given (CN = 4)
Matsui et al., 1982	$MgSiO_3$ liquid	MD simulation	2.1 Å (T > 5000 K?)
Kubicki and Lasaga, 1991	$MgSiO_3$ glass	MD simulation	1.9 Å (CN = 4) (T = 2000–5000 K)
This study	NaMg2 liquid	^{25}Mg NMR	est. 2.00 Å (1400 °C)
This study	CaMg2 liquid	^{25}Mg NMR	est. 2.08 Å (1400 °C)

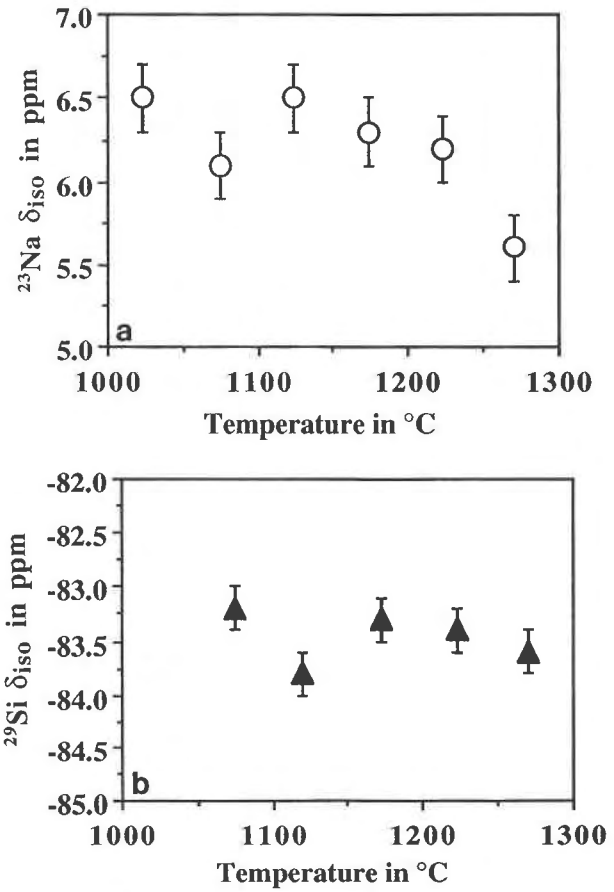

Fig. 8. (a) The ^{23}Na isotropic chemical shifts for NaMg2 liquid vs. temperature. (b) The ^{29}Si isotropic chemical shifts for NaMg2 liquid as a function of temperature.

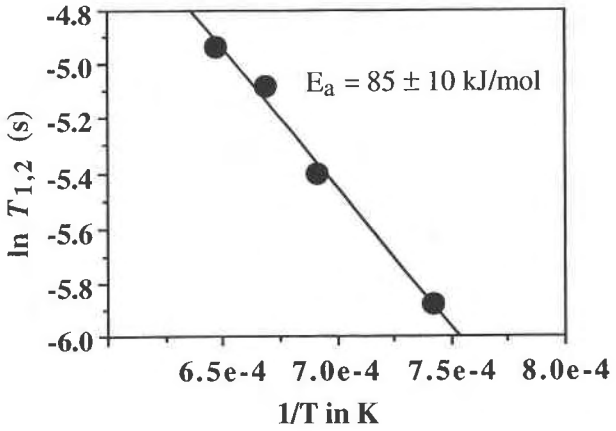

Fig. 9. The ^{23}Na NMR relaxation time data vs. temperature. An Arrhenius fit of these data yields an activation energy of 85 ± 10 kJ/mol.

increase in Si coordination in crystalline silicon phosphates and alkali silicophosphate glasses, but they ruled it out as an explanation for the concentration of [5]Si in alkali silicate glasses.

Temperature-dependent coordination environment of Mg

One of the most intriguing findings of this study is the strong temperature dependence in ^{25}Mg chemical shift in the sodium silicate liquid, from which data could be gathered over a range of temperature. Chemical shifts can change with temperature as a result of structural changes, as well as changes in the electronic character of the bonds with temperature. For ^{25}Mg, the latter effect has been carefully studied in MgO, where increased temperature causes a slight deshielding (+2 ppm from 25 to 1300 °C) attributed to the increased orbital overlap caused by thermal vibrations at high temperature (Fiske et al., 1994). The relatively large decrease in chemical shift with temperature observed for ^{25}Mg in the liquid is in the opposite direction than that caused by electronic effects and must therefore be caused by substantial changes in the structure of the liquid. In fact, the structural changes may be larger than observed if a temperature-dependent paramagnetic shift similar to that observed in MgO (Fiske et al., 1994) is subtracted.

In comparison with ^{25}Mg, the chemical shifts for ^{29}Si and ^{23}Na in the same liquid show much smaller changes: ^{29}Si chemical shifts remain constant, and ^{23}Na chemical shifts drop by about 1 ppm over the range of temperature studied. Recent high-temperature NMR studies of ^{29}Si, ^{27}Al, and ^{23}Na in alkali aluminosilicate liquids (Stebbins and Farnan, 1992) showed similarly small, but measurable, changes in the isotropic chemical shift for all these cations as a function of temperature.

Second-nearest-neighbor effects cannot be the dominant cause of these changes because a large change in the second-neighbor distribution around Mg should be evident as a temperature effect on δ_{iso} for ^{29}Si. Strong, three-dimensional clustering of Mg cations would lead to an increase in the average number of nonbridging O atoms per Si site (NBO/Si). We estimate that if the observed change in δ_{iso} for ^{25}Mg in the NaMg2 liquid is caused by a decrease in Mg clustering with increased T, the average NBO/Si would have to increase by about 0.2 over 300 °C. This should produce an easily observable change of 2 ppm in δ_{iso} for ^{29}Si. The lack of any detectable temperature effect for ^{29}Si thus suggests that local structural changes (coordination number and bond length) have the largest effect on the ^{25}Mg temperature dependence. Thus, the decrease in chemical shift with temperature most likely reflects changes in the local structure around Mg. If this temperature dependence persists down to reasonable glass transition temperatures for this composition (~600 °C), it may imply substantially smaller mean coordination numbers (roughly 4.5) and smaller Mg-O bond distances (1.95 Å) in the glass.

To compare the magnitude of the temperature-dependent structural changes for Mg with those observed for Si, Na, and Al, the measured chemical shift changes must be scaled relative to each other. Of all the structural parameters that can be correlated to chemical shifts, trends of coordination number vs. chemical shift are the most

TABLE 4. Relationships between bond lengths and chemical shifts for several cations in silicate minerals

Cation	Mineral	CN	M-O bond distance (Å)	δ_{iso} (ppm)	M-O/δ_{iso} (Å/ppm)	CN/δ_{iso} (CN/ppm)
Si	av. of 21 sites	4	1.63	−90	0.002	0.019
	av. of 5 sites	6	1.79	−195		
Al	av. of 14 sites	4	1.74	60	0.0032	0.038
	av. of 11 sites	6	1.91	7		
Na	β-$Na_2Si_2O_5$ (Na1)	4	2.42	15.6	0.013*	0.16
	β-$Na_2Si_2O_5$ (Na2)	6	2.45	9.4		
Mg	akermanite	4	1.915	49	0.004	0.05
	diopside (M1 site)	6	2.077	8		

* The stated value for ^{23}Na is based on 12 data points (Xue and Stebbins, 1993).

TABLE 5. Change in apparent coordination number for several cations based on high-T NMR and the relations between chemical shifts and bond lengths in Table 4

Cation	$\Delta\delta_{iso}$* (ppm/100 °C)	ΔCN** (per 100 °C)	Source
Si (in NaMg2) (1120–1370 °C)	0	0	this study
Na (in NaMg2) (1120–1370 °C)	−0.3	0.05	this study
Na (in NDS10AL-2) (1000–1340 °C)	−0.3	0.05	Stebbins and Farnan, 1992
Al (in NDS10AL-2) (500–1340 °C)	−0.6	0.02	Stebbins and Farnan, 1992
Mg (in NaMg2) (1120–1370 °C)	−1.7	0.09	this study

consistent [less so for ^{23}Na, for which δ_{iso} is very well correlated to the Na-O bond distance (Xue and Stebbins, 1993)]. Therefore, the measured $\Delta\delta_{iso}/\Delta T$ for ^{25}Mg, ^{29}Si, and ^{23}Na from this study and ^{29}Si, ^{27}Al, and ^{23}Na from the study of Stebbins and Farnan (1992) are divided by $\Delta\delta_{iso}/\Delta CN$ (where CN = coordination number) to provide a rough estimate of the change of mean apparent coordination number with temperature, $\Delta CN/\Delta T$. Using a mean value for the M-O bond distance for the cations in each coordination, an estimate of the M-O bond thermal expansion can also be calculated. The chemical shift data for ^{29}Si, ^{27}Al, ^{25}Mg, and ^{23}Na in representative coordinations are summarized in Table 4.

The results of this analysis are summarized in Table 5 and illustrated in Figure 10. Compared with other cations, Mg shows nearly three times as much structural change over a given interval of temperature as the other cations. The next-largest change is seen in Na. This may reflect some cooperative changes in coordination for both Na and Mg: since Si does not change its mean coordination by any measurable amount, the large structural change for Mg must necessitate some concomitant changes for Na.

One way to assess the effect of Mg coordination on Na coordination is to use simple Pauling bond-strength arguments for the cations and anions. For example, changing the coordination of Mg^{2+} from 4 to 6 lowers the nominal Mg-O bond strength by ⅙. The excess charge on the O atom caused by this coordination number increase could be offset by the addition of another Na to the coordination sphere around the O atom ($^{[6]}$Na-O bond strength = ⅙). That ^{23}Na NMR shows moderate lengthening of the Na-O bond may indicate that the changes associated with Mg^{2+} may actually involve some concomitant changes in Na-O bond length, as well as the addition of another Na^{1+} to the coordination of O. The relaxation time data also suggest some cooperative behavior between Mg^{2+} and Na^{1+} and will be discussed later.

The strong temperature dependence of Mg coordination may reconcile the results of this study at high temperature to the studies of glasses, which propose smaller mean coordination numbers for Mg. EXAFS studies of Fe^{2+} and Ni^{2+} (Waychunas et al., 1988; Jackson, 1991; Galoisy and Calas, 1991, 1992; Farges et al., 1993) showed that these cations are tetrahedrally coordinated in silicate liquids and glasses of similar composition to those in this study. In addition, the strong blue color of the glasses doped with Co^{2+} in this study suggests that Co^{2+} resides, at least partially, in tetrahedral coordination. Hanada et al. (1988) observed a similar coloration in Co^{2+}-doped glasses in the system MgO-SiO_2, which they interpreted to indicate $^{[4]}Co^{2+}$. Although divalent cations of similar size may not all reside in the same structural environment in silicate liquids and glasses (e.g., Williams et al., 1989; Cooney and Sharma, 1990; Keppler, 1992), the results of these studies have suggested to some workers that Mg^{2+}, being smaller than Fe^{2+}, and Co^{2+} may be more likely to be tetrahedrally coordinated in silicate glasses.

On the other hand, our results appear to disagree with recent high-temperature EXAFS and XANES studies of Ni in an alkali silicate glass and liquid, which suggested shorter Ni-O distances and a lower Ni coordination number in the latter phase (Farges et al., 1993). It may be that the behavior of Ni is somewhat different from that of Mg, that structural effects with T are highly nonlinear, or that NMR and X-ray absorption sample somewhat different aspects of the structure.

IMPLICATIONS FOR THERMOCHEMICAL AND TRANSPORT PROPERTIES OF MAGNESIUM SILICATE LIQUIDS

The strong temperature-dependent behavior of ^{25}Mg chemical shifts, if related to structural changes such as a mean coordination increase, should have significant implications for the physical and thermodynamic properties of magnesium silicate liquids. The partial molar heat capacity of MgO is the highest of any major oxide in silicate liquids, indicating that it has the strongest interaction with the network (Stebbins et al., 1984). Recent heat-capacity measurements of silicate liquids in the system MgO-Al_2O_3-SiO_2 suggest that the temperature-dependent structural changes taking place in the liquid involve changes in the local coordination environment of the cations (Courtial and Richet, 1993). Recent dilatometric and calorimetric

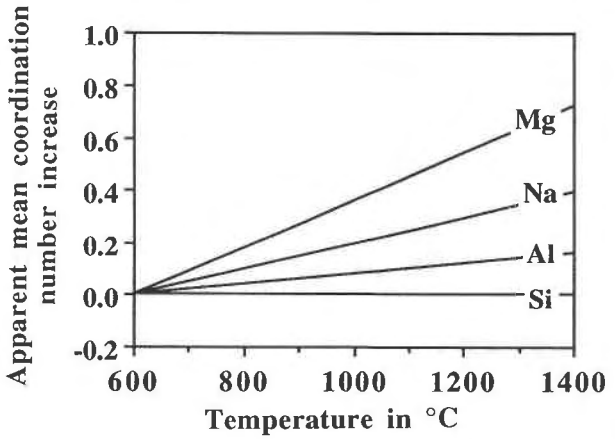

Fig. 10. Schematic representation of the relative structural change (e.g., apparent mean coordination number) for the cations in NaMg2 liquid based on observed changes in the chemical shifts for these cations vs. temperature from T_g. Data for ^{27}Al are also included from Stebbins and Farnan (1992).

determinations of thermal expansivity for silicate liquids in the system diopside-anorthite showed a strong decrease in the expansivity of the diopside composition with increasing temperature compared with anorthite (Knoche et al., 1992). This may indicate some temperature-dependent changes in cation coordination.

Our data also show significant compositional effects on Mg coordination. However, calculations of the partial molar heat capacity and volume of MgO in silicate melts have found constant values (e.g., Stebbins et al., 1984; Courtial and Richet, 1993; Lange and Carmichael, 1987, 1990). This may be because of the limited compositional and temperature range explored by existing bulk property measurements and the difficulty of measuring very Mg-rich liquids. For example, the most complete set of density data for silicate liquids (used to derive partial molar volumes and expansivities of the oxide components of natural silicate liquids) includes data for 13 Mg-bearing silicate liquids, most of which were Ca-rich (Lange and Carmichael, 1987). Only four samples contained any alkalis, and in these, the Ca to alkali ratio was >3.

An increase in mean Mg coordination with temperature may seem counterintuitive. Pressure, rather than temperature, is generally associated with coordination number increases for cations in silicate liquids (e.g., Xue et al., 1991). Strictly speaking, the ^{25}Mg chemical shift changes with temperature reflect a lengthening of the Mg-O bond, which may or may not lead to a discrete increase in the coordination number. Although the magnitude of Mg-O bond expansion with temperature is roughly three times larger than that observed in solids, it is consistent with the general expectation that bonds expand with temperature. Another explanation may be that the Mg environment in the liquid is becoming more symmetric with increasing temperature. Previous workers (e.g., Yin et al., 1983; Kubicki and Lasaga, 1991) have proposed that Mg may reside in a distorted octahedral site in $MgSiO_3$ liquid, with two O atoms at longer distances than the other four. MD simulations showed that the two longer Mg-O bonds correlate their vibrations so that one is closest to the Mg when the other is furthest away (Kubicki and Lasaga, 1991). A dynamical average of this environment might appear to be a net expansion of the site as a whole and a mean coordination number increase. For example, in the case of the mineral cryolite, the coordination number of the central Na atom increases from 8 to 12 at high temperature because of a dynamical averaging of the coordinating F atoms (Yang et al., 1993). However, it is unclear if this scenario would account for the configurational changes suggested by the thermochemical data for magnesium silicate liquids.

Lange and Carmichael (1987, 1990) have recently compiled data on molar volumes and thermal expansions of silicate liquids. They report a value for the temperature derivative of the partial molar volume of the MgO component, which, when divided by the partial molar volume, results in a value of 2.3×10^{-4}/K, which is roughly five times greater than the expansivity for crystalline MgO (e.g., Hazen and Finger, 1982). Although some or even most of this extra expansion in the liquid may take place through the rotation of cation polyhedra, its large value does suggest that additional mechanisms may be present.

An important difference between the effects of temperature on a liquid and those on most rigid solids is of course the greater range of structural configurations that ions can adopt in the former. As temperature increases in a silicate liquid, network modifiers in particular may begin to sample larger sites that are energetically relatively unfavorable because of longer bond lengths or charge imbalance. Some of these sites may be vacancy sites at low T; some may be large sites more frequently occupied by larger alkali cations. The effect on a bulk property such as molar volume or on an isotropic chemical shift results from the time-weighted average of all site occupancies.

Cation site exchange may have a particularly important role in the configurational entropy, enthalpy, and heat capacity of a liquid, particularly if exchange does occur with vacant sites. A close-packed O structure can serve as a crude starting point for estimating the possible magnitude of such effects. Such a structure contains two tetrahedral and one octahedral cation site per O. The mixing of cations on one-fourth to one-half of the larger sites could contribute 5–6 J/K per mole of O to the entropy of the liquid. This is a substantial fraction of the configurational entropy increase from the glass transition to the melting point of a composition such as $CaMgSi_2O_6$ [6.7 J/K per mole of O (Richet and Neuville, 1992)]. For a cation such as Mg^{2+} that may partially occupy tetrahedral sites, mixing onto octahedral vacancies could also be important, as could exchange with Si. It is likely that site exchange of network modifiers is closely coupled with silicate species exchange and Si-O bond breaking, which at least in high-silica liquids has been shown to be closely

tied to the mechanism of the transition from glass to liquid. We have only rather indirect evidence to support such speculations at this time, but such effects should be considered in models of melt thermodynamics. It is clear that these kinds of effect have the potential to contribute much more to the bulk properties of the liquid than does simple mixing of different coordinations of Mg, of $^{[4]}$Si and $^{[5]}$Si (Stebbins, 1991), or of Si species with varying numbers of bridging and nonbridging O atoms (Brandriss and Stebbins, 1988).

Dynamic behavior of Mg and Na

As stated earlier, NMR relaxation time measurements can yield information about the energetics of diffusive cation motion in materials (e.g., Stebbins, 1988). In the case of silicate liquids, the activation energies derived from NMR data may be in close agreement with those derived from measurements of macroscopic properties such as tracer diffusion and electrical conductivity (e.g., Liu et al., 1987, 1988).

The activation energy for Na relaxation derived from the ^{23}Na NMR data (85 kJ/mol) is in the same range as that measured in other compositions of approximately similar composition and degree of polymerization (e.g., $Na_2Si_2O_5$, 67 kJ/mol; $NaKSi_2O_5$, 95 kJ/mol; Liu et al., 1988). The fact that the activation energy determined in the NaMg2 silicate liquid is relatively high and similar to that for the mixed alkali disilicate liquids studied by Liu et al. (1988) may reflect a partial mixed-cation effect between the Na and the Mg.

The activation energy for Mg motion derived from the ^{25}Mg NMR data (119 kJ/mol) is intermediate between that of Na and that likely for Si under these conditions (170 kJ/mol: Farnan and Stebbins, 1990). Again, this implies that Mg seems to occupy some intermediate role in this silicate liquid, with diffusivities and bond strengths between that of the network-forming Si and network-modifying Na cations.

Few measurements of Mg tracer diffusion in silicate melts have been made. Thus, it is impossible to compare directly the relaxation time results with other data. However, MD simulation of Mg in $MgSiO_3$ and Mg_2SiO_4 liquids over a temperature range of approximately 2000–5000 K by Kubicki and Lasaga (1991) yield values of 76 and 97 kJ/mol, respectively. They are lower than those calculated for Si in these compositions but are probably higher than those for alkalis in liquids of similar polymerization.

Conclusions

The ^{25}Mg NMR spectra, although difficult to collect, can provide valuable information about the structural role of Mg in silicate minerals and liquids. The chemical shift range between $^{[4]}$Mg and $^{[6]}$Mg in silicate minerals may be somewhat larger than that observed in the oxides (Dupree and Smith, 1988), although further work is needed to refine this trend. The use of ^{25}Mg enriched samples, more sophisticated NMR pulse sequences, and, especially, higher magnetic fields may improve the applicability of ^{25}Mg NMR to a wider range of problems in mineralogy and geochemistry.

Whereas this study has been limited to simplified compositions and high temperatures, it has demonstrated that high-temperature NMR spectroscopy provides a means of investigating the specific structural contribution from each of the constituent cations that make up silicate liquids. The direct implications for the structural role of Mg in compositionally complex natural silicate liquids is uncertain at this point. For example, although the coordination number of Ti has been shown to be compositionally dependent in compositionally simple silicate liquids, it appears to be fixed over the compositional range of natural magmas. In the case of Mg, the compositional dependence on coordination might be similarly subdued, but the greater abundance of Mg in natural silicate liquids (particularly mafic compositions) may cause any structural variation to be physicochemically significant. A more detailed investigation of the partial molar volume of MgO in a wide range of natural and synthetic silicate liquids would help to answer this question.

Finally, it has been known for some time that silicate liquids must undergo structural changes with temperature. As most of what is known about the structure of silicate melts has come from the study of glasses, the structure of which represents that of the liquid at the glass transition (usually several hundred degrees below magmatic conditions), it is critical to assess the structural changes that take place as a function of temperature. This study documents a substantial change in the coordination of Mg with temperature and suggests that divalent cations such as Mg undergo the greatest change in local structure in silicate liquids with temperature. There is no evidence that the structural changes observed from 1100 to 1350 °C do not persist down to the glass transition. A determination of the coordination of Mg in these glasses (using Mg-EXAFS for example) would answer this question. In addition, high-temperature ^{25}Mg NMR studies of other compositions would also help to assess over what range of composition this temperature dependence is found.

References cited

Brandriss, M.E., and Stebbins, J.F. (1988) Effects of temperature on the structures of silicate liquids: ^{29}Si NMR results. Geochimica et Cosmochimica Acta, 52, 2659–2669.

Brown, G.E., Jr., Farges, F., Calas, G., Galoisy, L., Waychunas, G. A., Xu, N., Schwartz, K., and Dupon, R. (1993) High-temperature XAS studies of nucleation in glass-ceramics and of silica and germanate melt structure. Stanford Synchrotron Radiation Laboratory Proposal no. 2155M.

Cooney, T.F., and Sharma, S.K. (1990) Structure of glasses in the systems Mg_2SiO_4-Fe_2SiO_4, Mn_2SiO_4-Fe_2SiO_4, Mg_2SiO_4-$CaMgSiO_4$, and Mn_2SiO_4-$CaMnSiO_4$. Journal of Non-Crystalline Solids, 122, 10–32.

Coté, B., Massiot, D., Taulelle, F., and Coutures, J.-P. (1992) ^{27}Al NMR spectroscopy of aluminosilicate melts and glasses. Chemical Geology, 96, 367–370.

Courtial, P., and Richet, P. (1993) Heat capacity of magnesium aluminosilicate melts. Geochimica et Cosmochimica Acta, 57, 1267–1275.

Coutures, J.-P., Massiot, D., Bessada, C., Echegut, P., Rifflet, J., and

Taulelle, F. (1990) Etude par RMN ^{27}Al d'aluminates liquides dans le domaine 1600–2100 °C. Comptes Rendus de l'Academie des Sciences de Paris, 310, 1041–1045.

Dempsey, M.J., Kawamura, K., and Henderson, C.M.B. (1984) Molecular dynamics modelling of akermanite- and diopside-composition melts. Progress in Experimental Petrology, 6, 57–59.

Dingwell, D.B. (1992) Density of some titanium-bearing silicate liquids and the compositional dependence of the partial molar volume of TiO_2. Geochimica et Cosmochimica Acta, 56, 3403–3407.

Dingwell, D.B., and Webb, S.L. (1989) Structural relaxation in silicate melts and non-Newtonian melt rheology in geologic processes. Physics and Chemistry of Minerals, 16, 508–516.

——— (1990) Relaxation in silicate melts. European Journal of Mineralogy, 2, 427–449.

Dupree, R., and Smith, M.E. (1988) Solid-state magnesium-25 NMR spectroscopy. Journal of the Chemical Society: Chemical Communications, 1483–1485.

Engelhardt, G., and Michel, D. (1987) High-resolution solid-state NMR of silicates and zeolites, 485 p. Wiley, New York.

Farges, F., Brown, G.E., Jr., Calas, G., Galoisy, L., and Waychunas, G.A. (1993) High-temperature Xray absorption spectroscopy of Ni- and Ge in glasses and liquids (abs.). Eos, 74, 630.

——— (1994) Temperature-induced structural transformations in Ni-bearing silicate glass and melt. Geophysical Research Letters, in press.

Farnan, I., and Stebbins, J.F. (1990) High-temperature ^{29}Si NMR investigation of solid and molten silicates. Journal of the American Chemical Society, 112, 32–39.

Fiske, P.S., Stebbins, J.F., and Farnan, I. (1994) Bonding and dynamical phenomena in MgO: A high-temperature ^{17}O and ^{25}Mg NMR study. Physics and Chemistry of Minerals, in press.

Fukushima, E., and Roeder, S.B.W. (1981) Experimental pulse NMR: A nuts and bolts approach, 539 p. Addison-Wesley, Reading, Pennsylvania.

Galoisy, L., and Calas, G. (1991) Spectroscopic evidence for five-coordinated Ni in $CaNiSi_2O_6$ glass. American Mineralogist, 76, 1777–1780.

——— (1992) Network-forming Ni in silicate glasses. American Mineralogist, 77, 677–680.

——— (1993a) Structural environment of nickel in silicate glass/melt systems. I. Spectroscopic determination of coordination states. Geochimica et Cosmochimica Acta, 57, 3613–3626.

——— (1993b) Structural environment of nickel in silicate glass/melt systems. II. Geochemical implications. Geochimica et Cosmochimica Acta, 57, 3627–3633.

Ghose, S., and Tsang, T. (1973) Structural dependence of the quadrupole coupling constant e^2qQ/h for ^{27}Al and crystal field parameter D for Fe^{3+} in aluminosilicates. American Mineralogist, 58, 748–755.

Grandinetti, P.J., Baltisberger, J.H., Llor, A., Lee, Y.K., Werner, U., Eastman, M.A., and Pines, A. (1993) Pure absorption-mode lineshapes and sensitivity in two-dimensional dynamic-angle spinning NMR. Journal of Magnetic Resonance Series A, 103, 72–81.

Hanada, T., Soga, N., and Tachibana, T. (1988) Coordination state of magnesium ions in rf sputtered amorphous films in the system MgO-SiO_2. Journal of Non-Crystalline Solids, 105, 39–44.

Hazen, R.M., and Finger, L.W. (1982) Comparative crystal chemistry, 231 p. Wiley, New York.

Hovis, G.L., Spearing, D.R., Stebbins, J.F., Roux, J., and Clare, A. (1992) X-ray powder diffraction and ^{23}Na, ^{27}Al, and ^{29}Si MAS-NMR investigation of nepheline-kalsilite crystalline solutions. American Mineralogist, 77, 19–29.

Jackson, W.E. (1991) Spectroscopic studies of ferrous iron in silicate liquids, glasses and crystals, 162 p. Ph.D. thesis, Stanford University, Stanford, California.

Jackson, W.E., Mustre de Leon, J., Brown, G.E., Jr., Waychunas, G.A., Conradson, S.D., and Combes, J.-M. (1993) High-temperature XAS study of Fe_2SiO_4 liquid: Reduced coordination of ferrous iron. Science, 262, 229–233.

Janes, N., and Oldfield, E. (1985) Prediction of silicon-29 nuclear magnetic resonance chemical shifts using a group electronegative approach: Applications to silicate and aluminosilicate structures. Journal of the American Chemical Society, 107, 6769–6775.

Keppler, H. (1992) Crystal field spectra and geochemistry of transition metal ions in silicate melts and glasses. American Mineralogist, 77, 62–75.

Kirkpatrick, R.J. (1988) MAS NMR spectroscopy of minerals and glasses. In Mineralogical Society of America Reviews in Mineralogy, 18, 341–404.

Knoche, R., Dingwell, D.B., and Webb, S.L. (1992) Temperature-dependent thermal expansivities of silicate melts: The system anorthite-diopside. Geochimica et Cosmochimica Acta, 56, 689–699.

Kubicki, J.D., and Lasaga, A.C. (1991) Molecular dynamics simulation of pressure and temperature effects on $MgSiO_3$ and Mg_2SiO_4 melts and glasses. Physics and Chemistry of Minerals, 17, 661–673.

Kubicki, J.D., Hemley, R.J., and Hofmeister, A.M. (1992) Raman and infrared study of pressure-induced structural changes in $MgSiO_3$, $CaMgSi_2O_6$, and $CaSiO_3$ glasses. American Mineralogist, 77, 258–269.

Lange, R.L., and Carmichael, I.S.E. (1987) Densities of Na_2O-K_2O-CaO-MgO-FeO-Fe_2O_3-Al_2O_3-TiO_2-SiO_2 liquids: New measurements and derived partial molar properties. Geochimica et Cosmochimica Acta, 51, 2931–2946.

——— (1990) Thermodynamic properties of silicate liquids with an emphasis on density, thermal expansion and compressibility. Mineralogical Society of America Reviews in Mineralogy, 24, 25–64.

Lindsay, J., and Tossell, J. (1991) Ab initio calculations of ^{17}O and nT NMR parameters (nT = ^{31}P, ^{29}Si) in H_3TOTH_3 dimers and T_3O_9 trimeric rings. Physics and Chemistry of Minerals, 18, 191–198.

Lippmaa, E., Samoson, A., and Mägi, M. (1986) High-resolution ^{27}Al NMR of aluminosilicates. Journal of the American Chemical Society, 108, 1730–1735.

Liu, S., Pines, A., Brandriss, M., and Stebbins, J.F. (1987) Relaxation mechanisms and effects of motion in albite ($NaAlSi_3O_8$) liquid and glass: A high temperature NMR study. Physics and Chemistry of Minerals, 15, 155–162.

Liu, S., Stebbins, J.F., Schneider, E., and Pines, A. (1988) Diffusive motion in alkali silicate melts: An NMR study at high temperature. Geochimica et Cosmochimica Acta, 52, 527–538.

MacKenzie, K.J.D., and Meinhold, R.H. (1994a) Thermal reactions of crysotile revisited: A ^{29}Si and ^{25}Mg MAS NMR study. American Mineralogist, 79, 43–50.

——— (1994b) ^{25}Mg nuclear magnetic resonance spectroscopy of minerals and related inorganics: A survey study. American Mineralogist, 79, 250–260.

Matsui, Y., Kawamura, K., and Syono, Y. (1982) Molecular dynamics calculations applied to silicate systems: Molten and vitreous $MgSiO_3$ and Mg_2SiO_4 under low and high pressure. In S. Akimoto and M.H. Manghnani, Eds., High pressure research in geophysics: Advances in earth and planetary sciences, vol. 12, p. 511–524. Reidel, Boston, Massachusetts.

McMillan, P. (1984) A Raman spectroscopic study of glasses in the system CaO-MgO-SiO_2. American Mineralogist, 69, 645–659.

McMillan, P., Wolf, G., and Poe, B.T. (1992) Vibrational spectroscopy of silicate liquids and glasses. Chemical Geology, 96, 351–366.

Müller, D. (1982) Zur Bestimmung chemischer Verschiebungen der NMR-frequenzen bei Quadrupolkernen aus den MAS-NMR-spektren. Annalen der Physik, 39, 451–460.

Mysen, B.O., and Frantz, J.D. (1992) Raman spectroscopy of silicate melts at magmatic temperatures: Na_2O-SiO_2, K_2O-SiO_2, and Li_2O-SiO_2 binary compositions in the temperature range 25–1475 °C. Chemical Geology, 96, 321–332.

Navrotsky, A., Geisinger, K.L., McMillan, P., and Gibbs, G.V. (1985) The tetrahedral framework in glasses and melts: Inferences from molecular orbital calculations and implications for structure, thermodynamics, and physical properties. Physics and Chemistry of Minerals, 11, 284–298.

Navrotsky, A., Ziegler, D., Oestrike, R., and Maniar, P. (1989) Calorimetry of silicate melts at 1773 K: Measurement of enthalpies of fusion and of mixing in the system diopside-anorthite-albite and anorthite-forsterite. Contributions to Mineralogy and Petrology, 101, 122–130.

Paris, E., Dingwell, D.B., Romano, C., and Seifert, F.A. (1993) X-ray absorption study of Ti in silicate melts (abs.). Eos, 74, 347.

Richet, P., and Neuville, D.R. (1992) Thermodynamics of silicate melts: Configurational properties. In S.K. Saxena, Ed., Thermodynamic data: Systematics and estimation. Advances in Physical Geochemistry, 10, 132–161.

Risbud, S., Kirkpatrick, R.J., Taglialavore, A.P., and Montez, B. (1987) Solid-state NMR evidence of 4-, 5-, and 6-fold aluminum sites in roller-quenched SiO_2-Al_2O_3 glasses. Journal of the American Ceramic Society, 70, C10–C13.

Roedder, E.W. (1951) The system K_2O-MgO-SiO_2. I. American Journal of Science, 249, 81–130.

Rossman, G.R. (1988) Optical spectroscopy. In Mineralogical Society of America Reviews in Mineralogy, 18, 207–254.

Schairer, J.F. (1957) Melting relations of the common rock-forming oxides. Journal of the American Ceramics Society, 40, 215–235.

Schairer, J.F., and Bowen, N.L. (1942) The binary system $CaSiO_3$-diopside, and the relations between $CaSiO_3$ and akermanite. American Journal of Science, 240, 725–742.

Smith, K.A., Kirkpatrick, R.J., Oldfield, E., and Henderson, D.M. (1983) High-resolution silicon-29 nuclear magnetic resonance spectroscopy of rock-forming silicates. American Mineralogist, 68, 1206–1215.

Smyth, J.R., and Bish, D.L. (1988) Crystal structures and cation sites of the rock-forming minerals, 332 p. Allen and Unwin, London.

Stebbins, J.F. (1988) NMR spectroscopy and dynamic processes in mineralogy and geochemistry. In Mineralogical Society of America Reviews in Mineralogy, 18, 405–430.

——— (1991) Nuclear magnetic resonance at high temperature. Chemical Reviews, 91, 1353–1373.

Stebbins, J.F., and Farnan, I. (1992) Effects of high temperature on silicate liquid structure: A multinuclear NMR study. Science, 255, 586–589.

Stebbins, J.F., and McMillan, P. (1993) Compositional and temperature effects on five coordinated silicon in ambient pressure silicate glasses. Journal of Non-Crystalline Solids, 160, 116–125.

Stebbins, J.F., Carmichael, I.S.E., and Moret, L.K. (1984) Heat capacities and entropies of silicate liquids and glasses. Contributions to Mineralogy and Petrology, 86, 131–148.

Tossell, J., and Lazzeretti, P. (1987) Ab initio calculations of oxygen nuclear quadrupole coupling constants and oxygen and silicon NMR shielding constants in molecules containing Si-O bonds. Chemical Physics, 112, 205–212.

Waseda, Y. (1980) The structure of non-crystalline materials, 326 p. McGraw-Hill, New York.

Waseda, Y., and Toguri, J.M. (1977) The structure of molten binary silicate systems CaO-SiO_2 and MgO-SiO_2. Metallurgical Transactions, 8B, 563–568.

Waychunas, G.A., Brown, G.E., Jr., Ponader, C.W., and Jackson, W.E. (1988) Evidence from X-ray absorption for network-forming Fe^{2+} in molten alkali silicates. Nature, 332, 251–253.

Williams, Q., McMillan, P., and Cooney, T.F. (1989) Vibrational spectra of olivine composition glasses: The Mg-Mn join. Physics and Chemistry of Minerals, 16, 352–359.

Xue, X., and Stebbins, J.F. (1993) ^{23}Na chemical shifts and the local Na coordination environments in silicate crystals, melts and glasses. Physics and Chemistry of Minerals, 20, 297–307.

Xue, X., Stebbins, J.F., Kanzaki, M., McMillan, P.F., and Poe, B. (1991) Pressure-induced silicon coordination and tetrahedral structural changes in alkali oxide-silica melts up to 12 GPa: NMR, Raman, and infrared spectroscopy. American Mineralogist, 76, 8–26.

Yang, H., Ghose, S., and Hatch, D.M. (1993) Ferroelastic phase transition in cryolite, Na_3AlF_6, a mixed fluoride perovskite: High temperature single crystal X-ray diffraction study and symmetry analysis of the transition mechanism. Physics and Chemistry of Minerals, 19, 528–544.

Yin, C.D., Okuno, M., Morikawa, H., and Marumo, F. (1983) Structure analysis of $MgSiO_3$ glass. Journal of Non-Crystalline Solids, 55, 131–141.

Manuscript received January 26, 1994
Manuscript accepted May 24, 1994